2016

Modelling the response of phytoplankton to mesoscale and submesoscale processes at the Sub-Antarctic Front

Waring, Z.

Waring, Z. (2016) 'Modelling the response of phytoplankton to mesoscale and submesoscale processes at the Sub-Antarctic Front', The Plymouth Student Scientist, 9(2), p. 49-67.
http://hdl.handle.net/10026.1/14128

The Plymouth Student Scientist
University of Plymouth

*The Plymouth Student Scientist, 2016, **9**, (2), 49-67*

Modelling the response of phytoplankton to mesoscale and submesoscale processes at the Sub-Antarctic Front

Zoë E. Waring

Project Advisor Dr Jill Schwarz, School of Marine Science and Engineering, Plymouth University, Drake Circus, Plymouth, PL4 8AA

Abstract

This study extends a basic NPZ (Nutrient, Phytoplankton, Zooplankton) model to investigate the impact of turbulence on phytoplankton growth. Despite recent studies suggesting that submesoscale dynamics are crucial for the transfer of energy and nutrients across eddies, there are relatively few *in situ* studies and none, before now, at the Sub-Antarctic Front (SAF) to the East of Drake Passage. This study draws on data collected at the SAF and predictions made by the model to give an insight into the processes governing phytoplankton growth across a cold core mesoscale eddy. Conductivity, temperature, nutrient and chlorophyll-a (chl-a) measurements were used to assess physical and biological differences across the eddy. These were then compared to predictions made by the model to assess the response of phytoplankton to the dynamical conditions across the eddy. It was found that the turbulent conditions at the eddy boundary are likely to support a phytoplankton bloom, subsequently triggering an increase in zooplankton. Increased zooplankton levels cause an increase in grazing which is likely to enforce top down control, reducing phytoplankton numbers. The processes controlling growth within the eddy are not so well defined, however it is thought that phytoplankton growth is sustained, although growth in situ may have been limited by a micronutrient such as iron that was not included in the model. A lack of iron was also thought to be the cause of low levels of chl-a outside of the eddy as no other limiting factors were identified in measured or modelled data.

Introduction

Effects of turbulence at submesoscales

Turbulence plays an important role in the development of phytoplankton blooms (de Montera, et al., 2011). At very fine scales, turbulence influences the transfer of molecules between cells. Alternatively, turbulence, which operates over long scales in comparison to the size the organism, can bring together the key ingredients for sustaining life (nutrients and light) and cause large blooms to form (Estrada & Berdalet, 1997). This study focuses on the latter, in particular turbulence that is associated with submesoscale mixing at the boundary of a mesoscale eddy.

Submesoscale mixing is the result of lateral density gradients which occur within the surface mixed layer (SML) (Goncharov & Pavlov, 2001) which leads to the formation of fronts, filaments and eddies. Submesoscale circulations are observed at scales of 1-10 km and are formed within the top 100 m of the water column (Klein & Lapeyre, 2009). As they are smaller than mesoscale circulations they are crucial to the cascade of energy to micro- and finer scales (Lévy, et al., 2012). The dynamics created by submesoscales are important as they supplement the nutrient supply to the SML (Thomas, et al., 2008). With an abundance of nutrients being a crucial factor for triggering phytoplankton blooms (Estrada & Berdalet, 1997), submesoscales are consequently important for primary productivity in the pelagic ecosystem (Lévy, et al., 2001).

The effect that submesoscales have on the growth of phytoplankton depends on the factors which are initially limiting growth. For example, in oligotrophic environments, submesoscales may be responsible for as much as a third of new primary productivity (Lévy, et al., 2001), via the injection of nutrients into nutrient-depleted waters, although these turbulent movements may also be associated with downwelling which would have the negative effect of pulling phytoplankton out of the euphotic zone (Lévy, et al., 2012). In situations where nutrients are not limiting growth, submesoscales may still aid production by stratifying the water column. Stratification allows phytoplankton to remain in the euphotic zone allowing full utilisation of the available light and nutrients (Taylor & Ferrari, 2011). The extent to which these two scenarios occur is relatively under-studied (Lévy, et al., 2012). Observational data are particularly scarce; this prompted the SMILES (Surface Mixed Layer Evolution at Submesoscales) research project, the purpose of which is to gain a better understanding of the role that submesoscales have on changing the structure and properties of the upper ocean (Hosegood, et al., 2014). This aim is being addressed through observations made at the Sub-Antarctic Front (SAF) to the east of Drake Passage.

The SAF to the East of Drake Passage is an ideal location for the observation of both meso- and submesoscale dynamics due to the forcing of the Antarctic Circumpolar Current (ACC) through the narrowing at Drake Passage (Glorioso, et al., 2005). Instability at the SAF results in the formation of meanders and their subsequent eddies, leading to an increase in phytoplankton (Lévy, et al., 2001). The bathymetric features present at this location may also be affecting phytoplankton growth (Sokolov & Rintoul, 2007). It is thought that bathymetric features cause an increase in eddy kinetic energy, leading to an increase in fluid exchange (Thompson & Sallée, 2012). This can cause entrainment of limiting nutrients, such as iron, into

the euphotic zone. This is illustrated at frontal zones throughout the Southern Ocean (Sokolov & Rintoul, 2007). The water south of the SAF is formed of the Antarctic Surface Water (AASW), characterised by particularly cold, fresh water due to melt water originating from ice sheets (Talley, et al., 2011). The AASW has the potential to be high in the limiting nutrient Fe, as one potential source of Fe is precipitation accumulated upon the ice that, during the summer melting period, enriches the AASW (Death, et al., 2014). Consequently the mixing of AASW at the SAF can introduce Fe into iron-depleted waters, triggering blooms. However, depending on ice and wind conditions, phytoplankton blooms also occur within the marginal ice zone during austral spring (Smith & Nelson, 1985)and may deplete nutrients and iron in the AASW as it is being formed (Holm-Hansen, et al., 1994).

Apart from the recent SMILES cruise there have been no *in situ* studies of submesoscale processes in this region of the SAF, consequently it is important to examine the effects that these mixing processes are having on the availability of otherwise limiting nutrients and hence the effect on primary productivity of the region. Although the *in situ* data is unique and consequently important, it is impossible to fully appreciate the biological processes that are occurring by the measurements from a single research ship; it is therefore important to combine the measured data with predictions from biological models.

Phytoplankton modelling

To enhance the understanding of the dynamics within pelagic ecosystems, models have been developed to better understand the interactions between nutrients (N), phytoplankton (P) and zooplankton (Z). Such as NPZ models, these aim to describe the pelagic ecosystem based on chemical and biological fluxes (Fennel & Neumann, 2015). This approach means it is not necessary to consider separate species and individuals of zoo- and phytoplankton, instead they can be considered as a stock where the concentration varies depending on the variables and parameters (Miller, 2006). One of the most simplistic yet widely used NPZ model is that of Franks et al. (1986) (Eq. 1. a, b, c). In this model the variables are modelled in terms of nitrate, so for phytoplankton and zooplankton an estimate for the amount of nitrate per organism has to be assumed.

$$\frac{dP}{dt} = \frac{V_m N P}{K_s + N} - m_p P - Z R_m (1 - e^{-\Lambda P}) \quad (1.a)$$

$$\frac{dZ}{dt} = \gamma Z R_m (1 - e^{-\Lambda P}) - m_z Z \quad (1.b)$$

$$\frac{dN}{dt} = \frac{V_m N P}{K_s + N} + m_p P + m_z Z + (1 - \gamma) Z R_m (1 - e^{-\Lambda P}) \quad (1.c)$$

The interactions between the variables are as follows (refer to Table 1 for a glossary of terms): Nutrients are taken up by phytoplankton and converted to phytoplankton stock; this is represented by the Michaelis-Menton expression $(V_m N)/(K_s + N)$. The phytoplankton stock is then reduced by grazing zooplankton; the grazed phytoplankton is then converted to zooplankton tissue. The effect of grazing is represented by the Ivlev formula $R_m(1 - e^{-\Lambda P})$. Not all of the phytoplankton is converted to tissue some is lost due to metabolic processes and is excreted

appearing immediately as available nutrients. Both phytoplankton and zooplankton die and immediately appear as available nutrients (Franks, et al., 1986). These interactions are visualised by Fig. 1.

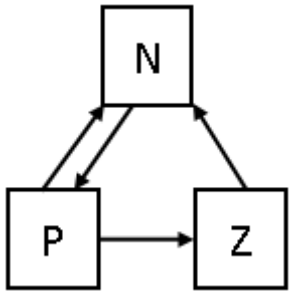

Figure 1: Box diagram for a NPZ (Nutrient, Phytoplankton and Zooplankton) model, arrows show the flow of nutrients within the system. Adapted from Franks, et al. (1986).

Despite being effective at modelling phytoplankton phenomena, such as the spring bloom cycles (Franks, et al., 1986) it is a simplistic approach which does not lend itself to the conditions observed at the SAF, such as the upwelling and downwelling associated with the front. The Franks et al. (1986) model is not equipped to deal with these issues as it assumes a sealed SML. A sealed SML forces the sum of the nutrient, phytoplankton and zooplankton stock to be constant, with only the proportions of each changing through time (Miller, 2006). A more realistic approach is to assume that nutrients will be mixed in and out of the SML and that some of the detritus will sink out. Other models have resolved this problem by converting to a two dimensional model and including terms for diffusion and advection (Edwards, et al., 2000). However, this increases the complexity of the model and the chances of finding false solutions in the model space. Relative simplicity is one of the advantages of the NPZ as the low number of parameters allows for easier exploration and understanding of model behaviour than with more complicated models (Franks, 2002).

Aims and objectives

This study explores the response of phytoplankton growth to dynamics associated with submesoscale and mesoscale features at the SAF.

The first aim of this study was to assess the changes in nutrient and chlorophyll-a (chl-a) concentrations across an eddy at the SAF. This was addressed by using temperature changes across an eddy at the SAF to identify three key areas: The Internal Zone (IZ), the External Zone (EZ) and the Boundary Zone (BZ). Nutrient and chl-a data were collected in these three areas and the variability of nutrients and chl-a within and between the three zones was characterised.

Secondly, the impact of turbulence associated with submesoscale dynamics on phytoplankton growth was investigated in greater detail using a model. This was addressed by extending a one dimensional NPZ model to include the effects of turbulence and simulating phytoplankton growth under varying turbulence representing the three eddy zones. A sensitivity analysis of the model was used, together with *in situ* data, to assign model parameter values.

Methods

In situ data collection

The distribution of nutrients and chl-a across a SAF eddy were assessed using data collected on board the RRS James Clark Ross as part of the SMILES research cruise. Firstly, the location of a newly formed cold core eddy was identified in SST data from the MODIS Aqua satellite. A towed, undulating body (SeaSOAR) equipped with temperature, salinity, conductivity and other sensors was then towed across the eddy at different locations around its perimeter, to form a total of 47 transects across the 60 km wide eddy (Fig. 2).

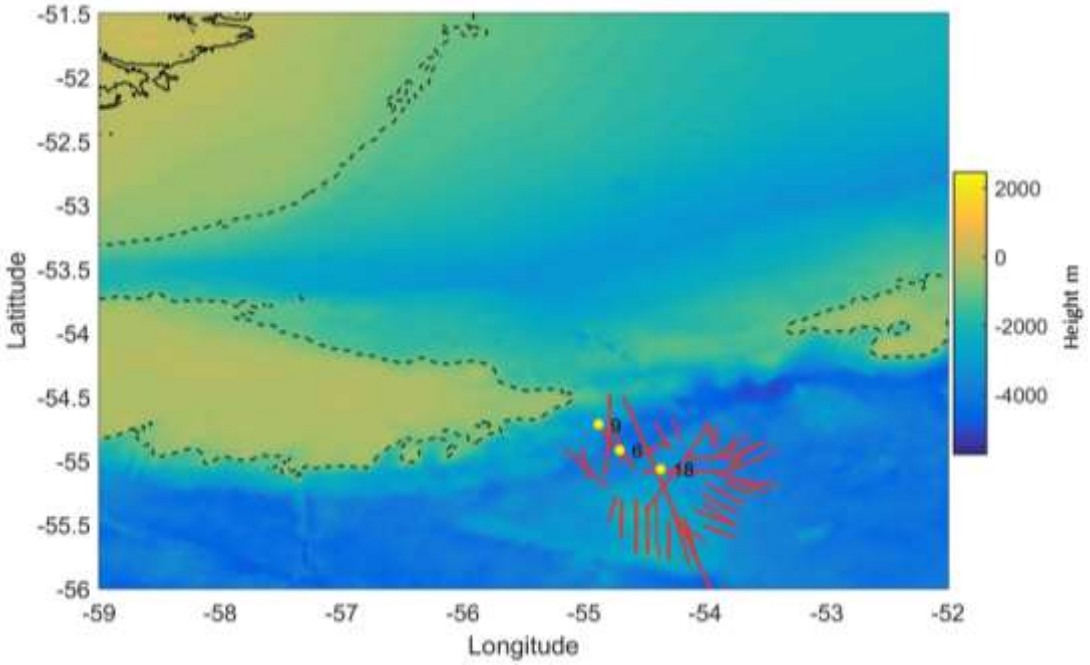

Figure 2: Bathymetry of the region (dashed line shows 1000m depth contour, solid line shows 0m depth contour), as well as location of SeaSOAR transects (red) and CTD stations 9, 6 and 18 (yellow).

During transects of the eddy, nutrient samples were collected from both the underway uncontaminated seawater (USW) supply and CTD rosette deployments. Once collected, the samples were filtered and frozen at -20°C, then analysed post-cruise for silicate, phosphate, ammonium and total nitrate. Chl-a was also measured throughout this period. Water from the USW supply was filtered, the filtrate extracted in 90% acetone using a Mini Beadbeater (Biospherical Instruments) and the eluent analysed fluorometrically for chl-a concentration using a Turner Trilogy fluorometer, calibrated against chl-a standard solutions (Sigma Aldrich).

The temperature data was used to identify three key areas; Internal Zone (IZ), External Zone and Boundary Zone, which were postulated to represent different turbulent mixing regimes. This enabled the nutrient and chl-a samples to be categorised based on their location within these three areas. The variability in nutrients and chl-a across these three locations was then statistically tested using t-tests for a significant difference between zones.

Numerical model

By introducing new assumptions to the original Franks, et al. (1986) model, the presented model addresses some of the key issues associated with the original parametrisation. The altered equations are shown below Eq. (2. a, b, c) see Table 1 for definitions of terms:

$$\frac{dP}{dt} = \frac{V_m NP}{K_s + N} - m_p P - ZR_m\left(1 - e^{-\Lambda(P-P_0)}\right) - T_u P \quad (2.a)$$

$$\frac{dZ}{dt} = \gamma ZR_m\left(1 - e^{-\Lambda(P-P_0)}\right) - m_z Z \quad (2.b)$$

$$\frac{dN}{dt} = \frac{V_m NP}{K_s + N} + m_p P + m_z Z + \frac{(1-\gamma)}{2} ZR_m\left(1 - e^{-\Lambda(P-P_0)}\right) - T_u N + T_u N_i \quad (2.c)$$

Table 1: Initial parameters and variables: Terms, definitions, values and the range of values used for the sensitivity analysis and the size of the step used within the range.

Term	Definition	Value	Analysis Range	Analysis Step
	Parameters			
V_m	Maximum phytoplankton growth rate	0.7 day^{-1}	0.525-0.875	0.035
K_s	Half saturation constant for nutrients	1µg N l^{-1}	0.75-1.25	0.05
m_p	Mortality rate of phytoplankton	0.1 day^{-1}	0.075-0.125	0.005
m_z	Mortality rate of zooplankton	0.2 day^{-1}	0.15-0.25	0.01
γ	Growth efficiency of zooplankton	0.3	0.225-0.375	0.015
R_m	Maximum grazing rate of zooplankton	1.5 day^{-1}	1.125-1.875	0.075
Λ	Ivlev constant	1.1 µg N l^{-1}	0.75-1.25	0.05
P_0	Phytoplankton threshold for grazing	0.2 µg N l^{-1}	0.15-0.25	0.01
T_u	Fractional turbulence rate	0.02 day^{-1}	0.015-0.025	0.001
N_i	Nutrient concentration below SML	0.3 µg N l^{-1}	0.225-0.375	0.015
	Variables			
N	Nutrient concentration	1.6 µg N l^{-1}		
P	Phytoplankton concentration	0.3 µg N l^{-1}		
Z	Zooplankton concentration	0.1 µg N l^{-1}		

The first assumption is zooplankton will only have the ability to graze above a critical concentration of phytoplankton. By changing the Ivlev formulation to $R_m(1 - e^{-\Lambda(P-P_0)})$, where P_0 is the critical threshold value, a threshold for grazing is achieved.

This adjustment prevents zooplankton from completely depleting the phytoplankton stock.

Instead of considering a sealed SML, the new model considers the effect of turbulence on the SML, all be it in a 1D sense:It is assumed that mixing will occur at a fractional rate, T_u, causing a percentage of water in the SML to be removed and to be replaced with water from below the SML. The removal of SML water, takes phytoplankton and nutrients out of the SML; it is then replaced with water of a constant nutrient concentration, N_i . The effect that turbulence will have on zooplankton is assumed to be negligible due to their ability to swim vertically.

Finally, the model now assumes the transformation of excreted matter from zooplankton into nutrients, is not instantaneous. Instead half of the excreted material (the sum of the zooplankton growth efficiency multiplied by the grazing rate) is added to the nutrient stock. The rest of this excreted material is assumed to sink out of the SML as detritus, after which it is no longer considered by the model.

These new dynamics are conceptualised in Figure 3. The flow of nutrients is depicted by the arrows and N, P, Z and Ni represent nutrients, phytoplankton, zooplankton and nutrients below the SML, respectively. Despite Ni having inputs and outputs it is assumed to be limitless and will remain at the same concentration.

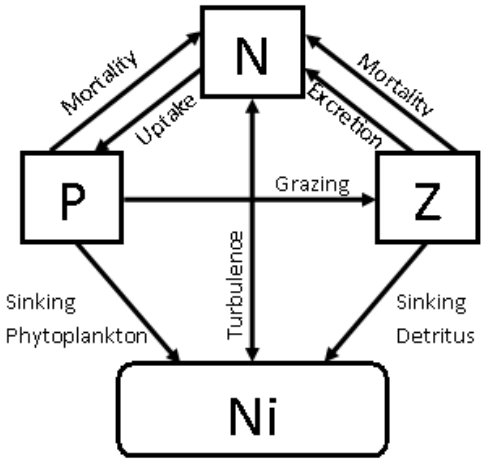

Figure 3: Conceptualisation of the new model, arrows indicates the flow of nutrients between N (nutrients), P (phytoplankton), Z (zooplankton) and Ni (nutrients below the SML) adapted from Franks et al. (1986).

Initial values for the parameters and variables are shown in Table 1. There is much debate in the literature regarding the exact values for these parameters, so where possible, the values used in the original Franks et al. (1986) model were used. This is due to the extent of the analysis undertaken to test the original model and its values, which demonstrated their suitability. The parameters which are not in the original model (P_0 , T_u , N_i ,) were assigned values based on the literature and observations made during the SMILES cruise. The model's sensitivity to initial conditions was analysed by considering a change of 25% in each individual parameter, in steps of 5%, either side of a central value (taken as the initial parameters; Table 1). The model's response to these changes was measured using the root mean square error (RMSE) compared to the central initial parameter value.

To study the changes across the eddy the model was run with varying turbulent (T_u= 0%, 1% and 4%) and initial nutrient (N = 1, 5, 10 µg Nl^{-1}) conditions, thus allowing the different zones of the eddy to be considered. The predictions could then be compared with:

- The CTD results, to establish whether mixing or stratification was dominant;
- Sampled nutrient data, to assess variations in increases or decreases across the eddy and
- Sampled chl-a data, to again assess variations.

Results and discussion

In situ measurements

The results from the SeaSOAR temperature and conductivity sensors (Fig. 4) identified that the eddy was a cold core eddy with internal temperatures close to 2^{o}C, compared to external temperatures above 4^{o}C. In the Southern Ocean, warm core eddies have been extensively studied for their impact on productivity (Ansorge, et al., 1999 and Kahru, et al., 2007. Cold core eddies have been studied to a lesser extent; nevertheless they have been shown to be important for primary production at the Gulf Stream (Lochte & Pfannkuche, 1987). Cold core eddies are important as they can lead to enhanced mixing and the upwelling of nutrients; conversely, they may cause stratification, allowing phytoplankton to remain in the euphotic zone (Lochte & Pfannkuche, 1987).

The edge of the eddy was well defined, due to the rapid temperature change over a relatively short distance (Fig. 4). By taking a sea surface temperature (SST) profile across the entire eddy, the three zones of the eddy could be defined by temperature (Table 2). Figure 4 illustrates the sample locations for nutrients and chl-a, the distribution of which is not even across all three zones. The BZ is particularly lacking *in situ* data, impacting on the quality of conclusions which can be drawn for the BZ; as well as impacting on the cross zone variance.

Table 2: Definition of eddy zones by temperature

Zone	Temperature Range ^{o}C
External	>3.7
Boundary	2.2-3.7
Internal	2-2.2

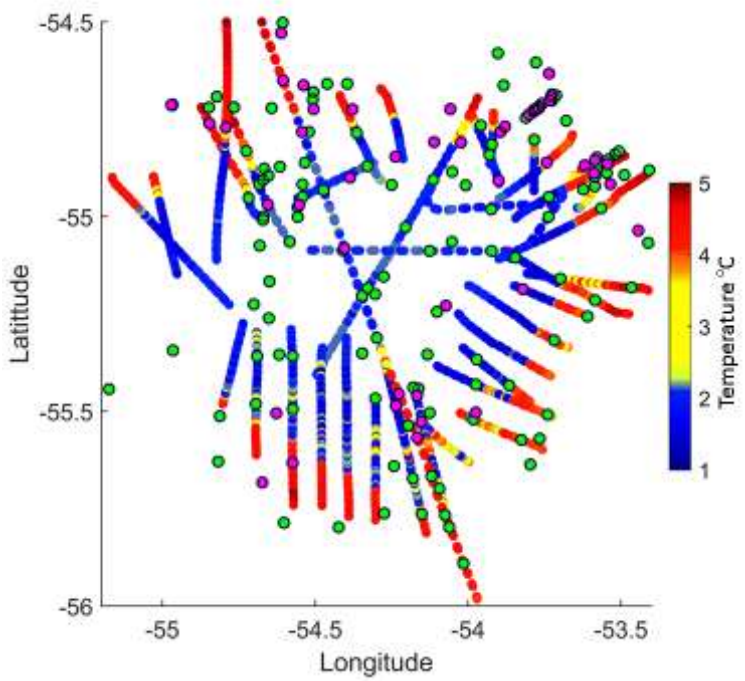

Figure 4: Change in temperature across the eddy measured by sensors on the towedSeaSOAR. Blue represents the IZ, yellow BZ and red EZ. Green plots show the locations of chl-a samples, magenta nutrient samples.

Vertical CTD profiles for temperature, salinity and density at the three zones (Fig 5), illustrate the differing levels of stratification. The IZ is the most stratified, with a four times greater change in density, from the surface to 200m, than the other two zones. This is due to a very cold fresh water input at 150m, which is characteristic of the Upper Circumpolar Deep Water (UCDW) (Orsi, et al., 1995); which would have been present at the SAF, when the eddy formed.

The BZ shows a steady increase in density over the 200m compared with the EZ which has a pycnocline between 110m and 130m. A steady increase in density is indicative of a mixed water column. Mixing is likely to be due to the submesoscale processes which were found to be present (Enriquez & Taylor, 2015). Consequently, it is assumed that the BZ will have the highest levels of turbulence. At the IZ, rotational forces act to elevate the pycnocline, (Fig. 5), trapping phytoplankton closer to the euphotic zone. A raised pycnocline can lead to an increase in productivity so long as nutrients are not depleted (Landry, et al., 2008).

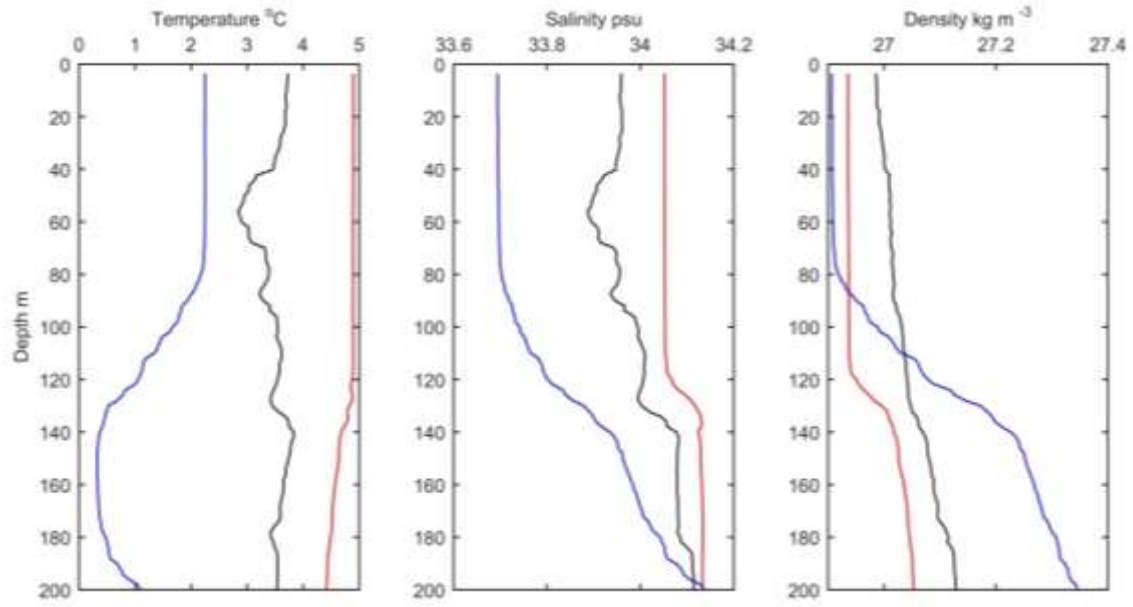

Figure 5: Vertical temperature salinity and density profiles from the CTD rosette, blue IZ, black BZ and red EZ.

Surface chl-a and nutrient values were compared between the three zones using analysis of variance (Fig. 6). The variation of chl-a was not found to be significant across the eddy, with a p-value of 0.83 (Table 3). As previously stated, the lack of *in situ* measurements restricts the power of this analysis. Nonetheless, the EZ has a lower range in chl-a values (Table 3), compared to the IZ (Table 3) illustrating that the IZ is effected by the physical dynamics found within the eddy. Physical processes within an eddy can create areas of upwelling and downwelling, leading to exchange of nutrients across the pycnocline and subsequent variations in chl-a levels. Alternately, a bloom could indicate stratification; causing phytoplankton to be held in the euphotic zone.

Table 3: Results of t-test, testing significant difference in chl-a between zones.

Chl-a	P value = 0.8305, N=6			
	Median	Min	Max	Range
EZ	0.242	0.233	0.26	0.027
BZ	0.243	0.162	0.266	0.104
IZ	0.2145	0.145	0.336	0.191

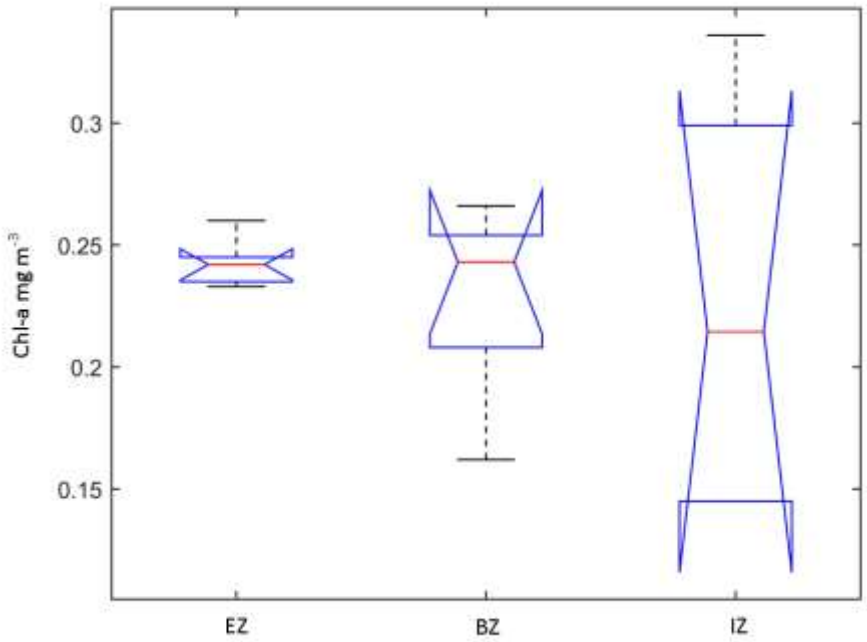

Figure 6: Measure of variance in chl-a across the three zones, P=0.83 N=6 at each zone.

Despite variation in the results none of the nutrients were found to be low enough to limit the growth of phytoplankton; consequently, reference to nutrients beyond this point will refer directly to total nitrate. Variance in the nutrient data (Fig. 7) implies there were lower nutrients at the IZ. Lower levels could be the result of depletion; however, without nutrient data from the pure IZ water source (the AASW) it is hard to certain. It is also possible that grazing occurred at the bloom before sampling, causing lower average chlorophyll concentrations (Table 3). This is certainly a possibility due to the preliminary results of the EK60 echo sounder, which suggests that grazing was strongest at the BZ, slightly lower within the eddy and lowest outside of the eddy (Roland Proud, pers. comm.). Although the analysis of variance for chl-a inferred a lack of zonation across the eddy, it does suggest a weak variation in nutrients, with a p-value of 0.1 (Table 4). Figure 7 suggests lower nutrient levels at the IZ. Low levels could be due to phytoplankton depleting the nutrient stock although, due to the wide range in values, it is hard to draw definitive conclusions. In comparison the spread of data at the BZ is smaller, which could be due to mixing associated with the front sustaining a constant supply of nutrients.

Table 4: Results of t-test, testing significant difference in nutrients between zones.

Nut	P value = 0.0991, N=6			
	Median	Min	Max	Range
EZ	24.24	21.81	31.43	9.62
BZ	24.745	22.72	25.11	2.39
IZ	23.425	14.47	24.43	9.96

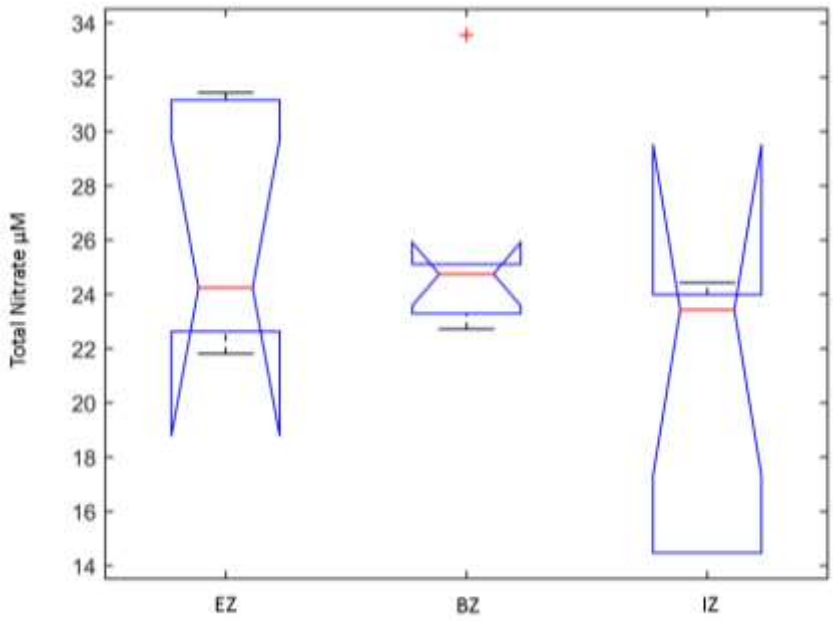

Figure 7: Measure of variance in nutrients across the three zones, P=0.1, N=6 at each zone.

Modelled predictions

Compared with predictions from the original model (Franks, et al., 1986) (Fig. 8), the plankton threshold (first 100 days of Fig. 9) is proven to be effective, as it prevents the oscillatory boom and bust cycles. By allowing the development of an initial bloom followed by equilibrium, the model predicts a more realistic scenario (Miller, 2006). After 100 days, turbulence was introduced, at a rate of 2%. This caused an increase in available nutrients which triggered a second bloom, this in turn triggered grazing after which biomass levels remained relatively low. This is characteristic behaviour of bloom cycles which was first discussed by Evans and Parslow (1985), whereby the first winter storms cause mixing, introducing nutrients into the depleted SML. However, continual mixing over winter removes phytoplankton from the SML preventing further blooms, until calmer conditions in spring causes stratification of the SML triggering another bloom.

The stability analysis revealed that the nutrient variable was particularly sensitive to changes in the initial parameter values (Table 5). A 5% change in some parameters led to as much as a 10 fold variation in nutrient concentration. This instability is likely to be due to the output being dependant on changes in both phytoplankton and zooplankton concentrations. Because phytoplankton and zooplankton did not vary to the same extent (all of the 5% parameter variations produced outputs that were one third, or less, than their initial parameter outputs), the model is considered to be stable. To validate this, more *in situ* data needs to be collected to test whether the large variation in nutrients represents reality. Alternatively, a 2D model could be used to better resolve turbulence thus producing better predictions for the changes in nutrients.

Table 5: RMSE results (% change in N, P, Z) for 25% variation from initial parameter value in steps of 5%

Term	N	P	Z
Vm	1951.93	23.95	28.60
Tu	163.69	6.48	9.02
Rm	1448.34	10.32	5.06
P0	1117.82	9.19	17.85
Ni	413.68	10.23	10.21
mz	2330.57	33.08	28.92
mp	54.03	3.41	6.83
lambda	1128.67	10.87	21.92
Ks	2.78	0.99	2.06
gamma	1527.03	9.82	5.48

To compare the effects of changing turbulence across the eddy the model was run with 0%, 1% and 4% turbulence exchange rates over a period of 30 days (Fig. 10. a, b, c). At 4% the model predicts the biggest bloom which reaches a maximum of 3.75µg Nl^{-1} after 11 days. This is greater than the 1% and 0% runs, which reached 2.08 µg Nl^{-1} after 9 days and 1.58 µg Nl^{-1} after 8 days, respectively. The bloom which was induced in the 4% run then proceeded to decrease to a minimum of 0.68 µg Nl^{-1} on day 21 and then increased to 1.09 µg Nl^{-1} over the remaining 9 days. This second rise is not of the same magnitude as the initial bloom, despite nutrient concentrations being higher (3.87 µg Nl^{-1} compared with 1.97 µg Nl^{-1}). Increased zooplankton levels may contribute to the low levels of phytoplankton in the second growth event. This is likely to be due to the zooplankton increase after the phytoplankton bloom indicating that the low levels of phytoplankton were at least partly due to grazing and the effects of top down control. Low levels may also have been due to the removal of phytoplankton via turbulence. The run finishes with classic Southern Ocean characteristics of high nutrients and low phytoplankton levels (Falkowski, et al., 1998). When the model is left for a longer period the nutrient level continues to rise. This is likely to be due to the addition of nutrients, through turbulence, with every time step. To prevent an infinite amount of nutrient entering the system, a cap could be implemented; it should be set to prevent concentrations exceeding that of below the SML. In comparison, the phytoplankton in the 1% run decreased to 0.89 µg Nl^{-1} before increasing to 1.01 µg Nl^{-1}. The nutrient concentration dropped to a similar amount as in the 4% run, however it did not increase to the same extent after the bloom. Instead, it increased to 1µg Nl^{-1}, a similar level as the phytoplankton at that time. This limited nutrient increase is due to the reduced mixing which is introducing fewer nutrients to the system.

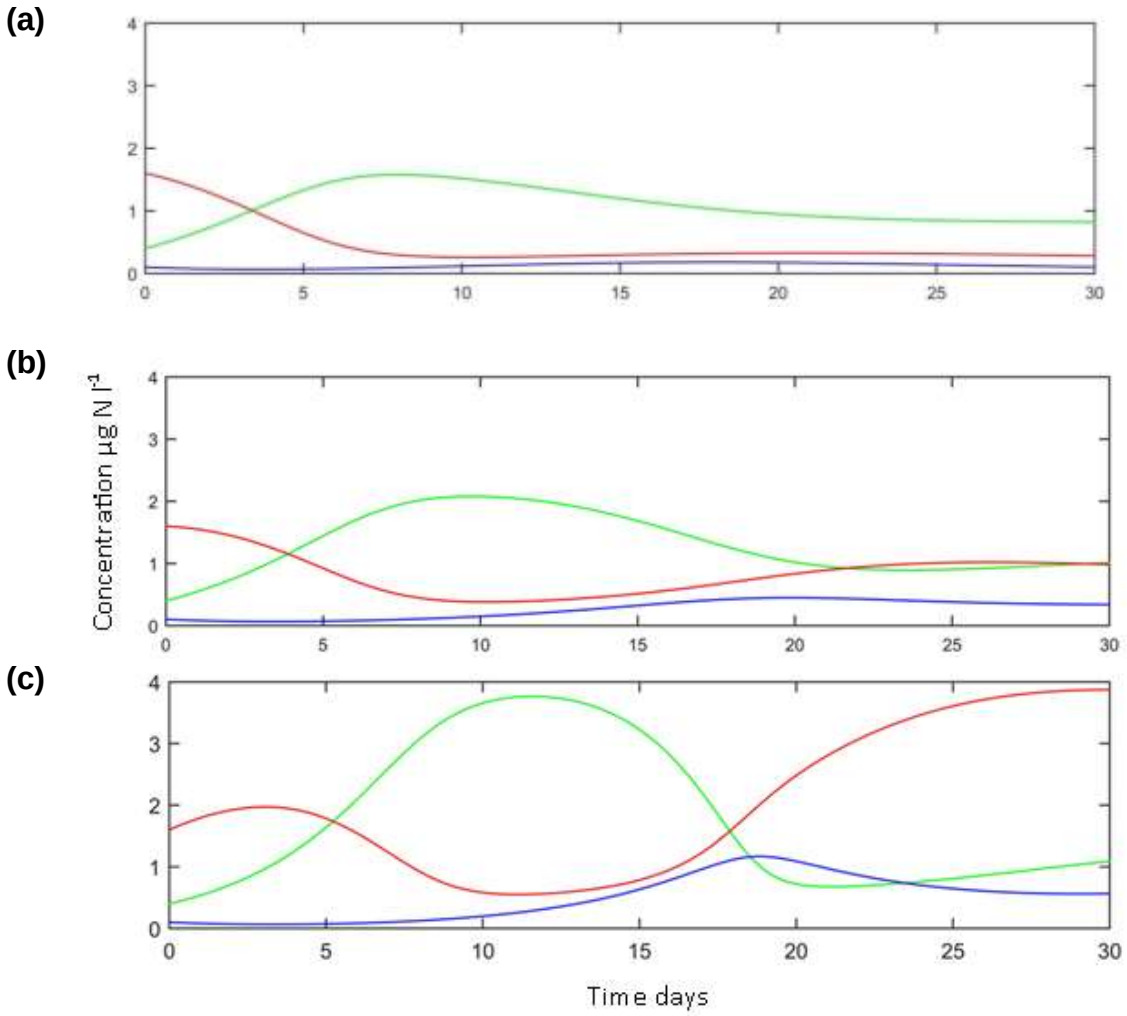

Figure 10: Modelled change in phytoplankton (green), nutrients (red) and zooplankton, with turbulence set at 0% (a), 1% (b) and 4% (c).

To examine the effect of different initial nutrient levels, the model was run with turbulence set at 1% for high (10 µg Nl^{-1}), moderate (5 µg Nl^{-1}) and low (1 µg Nl^{-1}) nutrient scenarios (Fig. 11. a, b, c,). The high nutrient scenario triggered the largest phytoplankton bloom, whereas the low nutrient scenario failed to trigger a substantial bloom; instead phytoplankton levels slowly rose to 1.77 µg Nl^{-1} before slowly declining. Despite the higher nutrient levels triggering blooms to develop, all three runs finished with very similar values (0.94 µg Nl^{-1} for high nutrient, 1.06 µg Nl^{-1} for moderate nutrient, 0.96 µg Nl^{-1} for low nutrient). Nutrients do not appear to be a limiting factor at this point, particularly for the high nutrient run, as the end nutrient concentration was 3.33 µg Nl^{-1}, which is higher than the initial value for the low nutrient run, so that bloom control by zooplankton must be considered. The zooplankton concentration at the end of the high nutrient run was nearly twice as much as that at the end of the low nutrient run (0.62 µg Nl^{-1} compared with 0.35 µg Nl^{-1}). The higher zooplankton levels are a result of increased grazing during the bloom; because the low nutrient run never experienced a bloom, zooplankton has not been able to graze sufficiently to increase in number. Lower zooplankton levels allowed phytoplankton to reach the same concentration as the high nutrient run, but

with a third of the available nutrients, suggesting that top down control was the dominant factor.

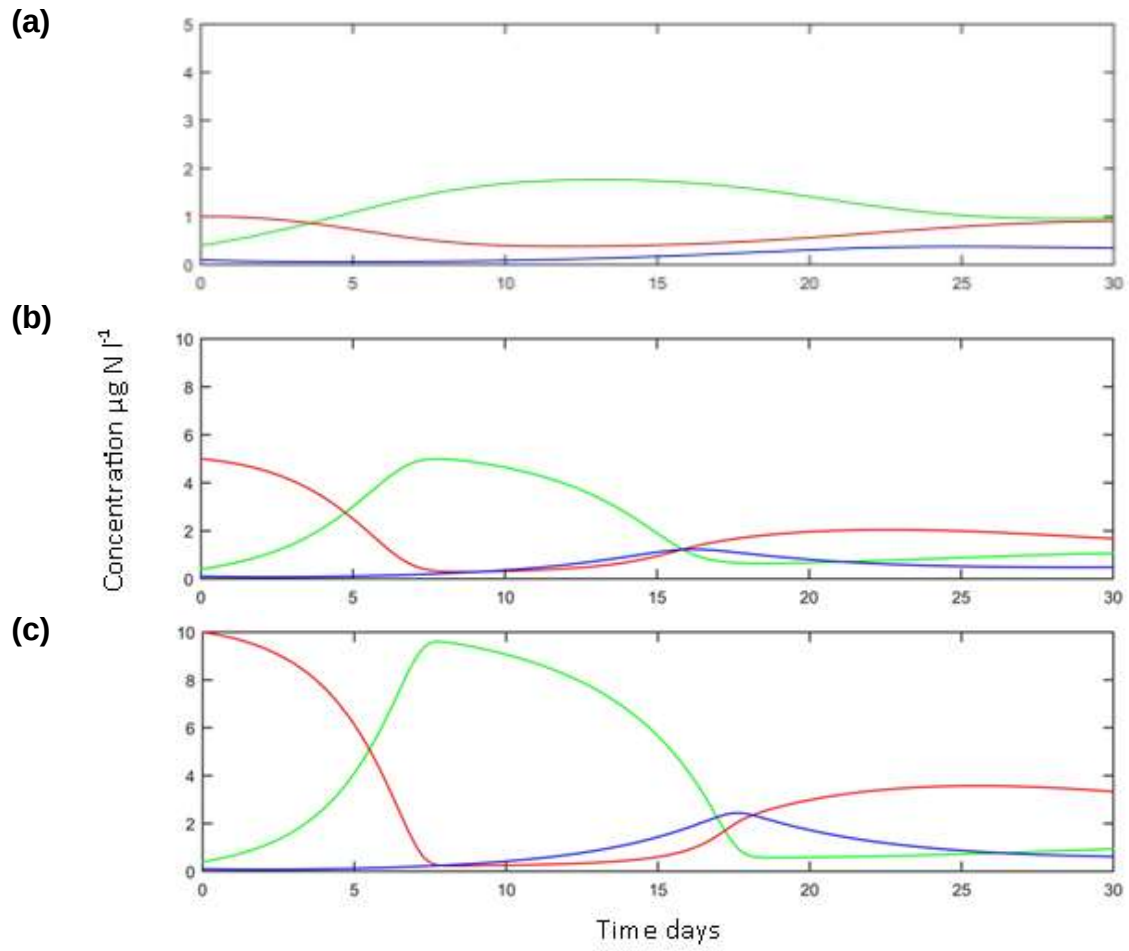

Figure 11: Modelled change in phytoplankton (green), nutrients (red) and zooplankton, initial nutrients set at 1 µg Nl^{-1} (a), 5 µg Nl^{-1} (b) and 10 µg Nl^{-1} (c).

Phytoplankton growth across the eddy

Predictions made by the model can be used to consider the processes controlling the growth of phytoplankton across the eddy zones. The EZ is likely to be at equilibrium during sampling, as the water has not been subjected to major changes in levels of turbulence. Reaching equilibrium could be the cause of the very small spread in chl-a data. Nutrient results show the spread of data was generally higher in the EZ, suggesting that nutrients were not limiting phytoplankton growth. Preliminary results for zooplankton suggest abundance was low at the EZ (Roland Proud, pers. comm.) eliminating the chance of top down control; therefore there must be another limiting factor that has not been considered. A low abundance of a micro nutrient, such as Fe, which was not measured during sampling, could limit growth. Fe has been shown to be a limiting factor in the Southern Ocean (Martin, et al., 1990 and Martínez-García & Winckler, 2015) and could explain the HNLC (High Nutrient Low Chlorophyll) characteristics.

If the BZ is assumed to be dominated by turbulence, the model implies a large bloom would develop and subsequently decline due to grazing. Turbulent processes within

the BZ could lead to an increase in micro nutrients, such as Fe, which could be limiting growth. The preliminary results for zooplankton suggest that grazing was enhanced at the BZ (Roland Proud, pers. comm.). Enhanced grazing at the BZ coincides with predictions from the model; which suggests, areas of higher turbulence will have higher levels of zooplankton. Nutrients within the BZ were measured to be slightly higher than in the other zones; alluding to the start of the secondary increase in nutrients, during the high turbulence model run (Fig. 10.c).

It is hard to determine from the data set whether turbulent conditions exist in the IZ. Despite CTD profiles suggesting stratification, a very wide spread of nutrient data suggests turbulence is causing upwelling of nutrients or a certain degree of phytoplankton growth is depleting the nutrient stock. To further understand the availability of nutrients at the IZ the origins of the water need to be considered. As previously discussed the IZ water, originated from waters south of the SAF; studies have shown that the ASW may be limited in a micro nutrient such as Fe (Klunder, et al., 2010), causing bottom up control.

Further study

A factor which is not directly considered by the model is the impact of nutrient recycling by the microbial loop. The microbial loop plays a key role in marine ecosystems as bacteria feed upon DOM (Dissolved Organic Matter), bacteria is then grazed upon by protozoa, which are grazed by zooplankton (Azam, 1998 and Fenchel, 2008). The implications of the microbial loop are an area of intense research; findings indicate that it is a key dynamic in the evolution of marine food webs (Fuhrman, et al., 2015). Consequently models which aim to have a complete overview of the marine ecosystem must consider the effects of the loop (Chaalali, et al., 2015). The model may also be extended by exploring the effects of turbulence further. The possibility of doing so in a 1D context is limited, instead the biological aspect of the model could be coupled with an advanced physical model. The coupling of models is advantageous as it can gain insight to how biological dynamics are affected by varying scales of 3D mixing (Watteaux, et al., 2015 and Enriquez & Taylor, 2015). Other areas for consideration include the effect of seasons which have been shown to be critical for phytoplankton growth in the Southern Ocean (Philibert, et al., 2015), as well as the degradation of light with depth and the interaction this has with a changing SML depth (Huisman, et al., 1999).

Conclusion

This study assessed the changes in nutrients and chl-a across a cold core eddy generated at the SAF; the findings were attained through *in situ* measurements and predictions made by an extended NPZ model. The BZ was shown to have increased turbulence, demonstrated by the CTD profiles; the model predicts that increased turbulence will cause initial increases in phytoplankton, triggering enhanced grazing by zooplankton. The chl-a, nutrient and preliminary zooplankton data give evidence to support the predictions made by the model; although the evidence is limited by the low number of *in situ* measurements. Low levels of measurements make it hard to define the dominant conditions at the IZ; however there is evidence of phytoplankton growth, accounted for by the wide spread in both nutrient and chl-a data and the moderate amount of grazing. The measurements at the IZ suggest some form of physical process aiding phytoplankton growth, albeit to a lesser extent than that at

the BZ. Findings suggest the EZ was at equilibrium, due to the very small range in chl-a values. There was no evidence that the nutrients tested were limiting phytoplankton growth or that zooplankton were causing down control, signifying that a limiting nutrient, such as Fe, may have prevented phytoplankton growth. Overall the model was well suited to predicting the long term impacts of turbulence on phytoplankton growth and demonstrates the potential that turbulent movements, which are a result of submesoscale processes, have a positive impact on the growth of phytoplankton.

Acknowledgements
First and foremost I would like to take the opportunity to thank my supervisor Dr Jill Schwarz, for all of her support and encouragement over the course of this project. Gratitude also goes to Dr Phil Hosegood, who provided the opportunity to take part in the SMILES research cruise- a truly inspiring experience. Thanks are also extended to the crew of the RRS James Clarke Ross and to Malcolm Woodward (Plymouth Marine Laboratory), for analysing the nutrient samples.

References

Ansorge, I. J. et al., 1999. Physical-biological coupling in the waters surrounding the Prince Edward Islands (Southern Ocean). *Polar Biology*, 21(3), pp. 135-145.

Azam, F., 1998. Microbial control of oceanic flux: The plot thickens. *Science*, 280(5364), pp. 694-696.

Chaalali, A. et al., 2015. A new modeling approach to define marine ecosystems food-web status with uncertainty assessment. *Progress in Oceanography,* 135, pp. 37-47.

de Montera, L. et al., 2011. Multifractal analysis of oceanic chlorophyll maps remotely sensed from space. *Ocean Science*, 7, 219-229.

Death, R. et al., 2014. Antarctic ice sheet fertilises the Southern Ocean. *Biogeosciences*, 11(10), pp. 2635-2643.

Edwards, C. A., Powel, T. A. & Batchelder, H. P., 2000. The stability of an NPZ model subject to realistic levels of vertical mixing. *Journal of Marine Research*, 58, pp. 37-60.

Enriquez, R. M. & Taylor, J. R., 2015. Numerical simulations of the competition between wind-driven mixing and surface heating in triggering spring phytoplankton blooms. *ICES Journal of Marine Science*, 72(6), pp. 1926-1941.

Estrada, M. & Berdalet, E., 1997. Phytoplankton in a turbulent world. *Scientia Marina*, 61(1), pp. 125-140.

Evans, G. T. & Parslow, J. S., 1985. A model of plankton cycles. *Biological Oceanography*, 3(3), pp. 327-347.

Falkowski, P. G., Barber, R. T. & Smetacek, V., 1998. Biogeochemical Controls and Feedbacks on Ocean Primary Production. *Science*, 281(5374), pp. 200-206.

Fennel, W. & Neumann, T., 2015. *Introduction to the Modelling of Marine Ecosystems*. 2nd ed. Amsterdam: Elsevier.

Fenchel, T., 2008. The microbial loop- 25 years later. *Journal of Experimental Marine Biology and Ecology*, 366(1-2), pp. 99-103.

Franks, P. J. S., 2002. NPZ Models of Plankton Dynamics: Their Construction, Coupling to Physics, and Application. *Journal of Oceanography*, 58(2), pp. 379-387.

Franks, P. J. S., Wroblewski, J. S. & Flierl, G. R., 1986. Behaviour of a simple plankton model with food-level aclimation by herbivores. *Marine Biology*, 91, pp. 121-129.

Fuhrman, J. A., Cram, J. A. & Needham, D. M., 2015. Marine microbial community dynamics and their ecological interpretation. *Nature Reviews Microbiology*, 13, pp. 133-146.

Glorioso, P. D., Piola, A. R. & Leben, R. R., 2005. Mesoscale eddies in the Subantarctic Front - Southwest Atlantic. *Scientia Marina*, 69(2), pp. 7-15.

Gomez-Enri, J., Quartly, G. D., Navarro, G. & Villares, P., 2007. *Characterizing and following eddies in Drake Passage*. Univ Cadiz, Cadiz, Conference: Geoscience and Remote Sensing Symposium, IEEE international.

Goncharov, V. & Pavlov, V., 2001. Cyclostrophic vortices in polar regions of rotating planets. *Nonlinear Processes in Geophysics*, 8, pp. 301-311.

Holm-Hansen, O. et al., 1994. n situ evidence for a nutrient limitation of phytoplankton growth in pelagic Antarctic waters. *Antarctic Science*, 6(03), pp. 315-324.

Hosegood, P. J., Sallee, J. B. & Torres, R., 2014. Description of proposed research.

Huisman, J., van Oostveen, P. & Weissing, F. J., 1999. Critical depth and critical turbulence: Two different mechanisms for the development of phytoplankton blooms. *Limnology and Oceanography*, 44(7), pp. 1781-1787.

Kahru, M., Mitchell, B. G., Gille, S. T. & Hewes, C. D., 2007. Eddies enhance biological production in the Weddell-Scotia Confluence of the Southern Ocean. *Geophysical Research Letters*, 34(14).

Klein, P. & Lapeyre, G., 2009. The Oceanic Vertical Pump Induced by Mesoscale and Submesoscale Turbulence. *Annual Review of Marine Science*, 1, pp. 351-357.

Klunder, M. B. et al., 2010. Dissolved iron in the Southern Ocean (Atlantic sector). *Deep-Sea Research II*, 58, pp. 2678-2694.

Lévy, M., Klein, P. & Treguier, A., 2001. Impact of sub-mesoscale physics on production and subduction of phytoplankton in an oligotrophic regime. *Journal of Marine Research*, 59, pp. 535-565.

Lévy, M. R. et al., 2012. Bringing physics to life at the submesoscale. *Geophysical Research Letters*, 39(14), L14602.

Lochte, K. & Pfannkuche, O., 1987. Cyclonic cold-core eddy in the eastern North Atlantic. ii. Nutrients, phytoplankton and bacterioplankton. *Marine Ecology*- progress series, 39, pp. 153-164.

Martin, J. H., Gordon, R. M. & Fitzwater, S. E., 1990. Iron in Antarctic waters. *Nature*, 345(6271), pp. 156-158.

Martínez-García, A. & Winckler, G., 2015. Iron fertilization in the glacial ocean. *DUST*, 24, p. 82.

Miller, C. B., 2006. *Biological Oceanography*. 4 éd. Oxford: Blackwell Science Ltd.

Moore, K. & Abbott, M. R., 2000. Phytoplankton chlorophyll distributions and primary production in the Southern Ocean. *Journal of Geophysical Research*, 105(C12), pp. 28,709-28,722.

Nihoul, J. C., 1975. Modelling of marine systems. *Elsevier Oceanography Series*, 10 ed. Oxford: Elsevier.

Orsi, A. H., Whitworth, T. & Nowlin Jr, W. D., 1995. On the meridonal extent and fronts of the Antarctic Circumpolar Current. Deep Sea Research Part I: *Oceanographic Research Papers*, 42(5), pp. 641-673.

Philibert, R., Waldron, H. & Clark, D., 2015. A geographical and seasonal comparison of nitrogen uptake by phytoplankton in the Southern Ocean*. Ocean Science*, 11, pp. 251-267.

Smith, W. O. & Nelson, D. M., 1985. Phytoplankton bloom produced by a receding ice edge in the Ross Sea- spatial coherence with the density field. *Science*, 227(4683), pp. 163-166.

Sokolov, S. & Rintoul, S. R., 2007. On the relationship between fronts of the Antarctic Circumpolar Current and surface chlorophyll concentrations in the Southern Ocean. *Journal of Geophysical Research*, 112(C7), pp. 1-17.

Talley, L. D., Pickard, G. L., Emery, W. J. & Swift, J. H., 2011. *Descriptive Physical Oceanography*. 6th ed. London: Elsevier.

Taylor, J. R. & Ferrari, R., 2011. Ocean fronts trigger high latitude phytoplankton blooms. *Geophysical Research Letters*, 38, L23601.

Thomas, L. N., Tandon, A. & Mahadevan, A., 2008. Submesoscale Processes and dynamics. *Ocean Modelling in an Eddying Regime*, pp. 17-38.

Thompson, A. F. & Sallée, J. B., 2012. Jets and Topography: Jet Transitions and the Impact on Transport in the Antarctic Circumpolar Current. *American Meteorological Society*, 42, pp. 956-972.

Watteaux, R., Stocker, R. & Taylor, J. R., 2015. Sensitivity of the rate of nutrient uptake by chemotactic bacteria to physical and biological parameters in a turbulent environment. *Journal of Theoretical Biology*, 387, pp. 120-135.